Journal of Materials Chemistry C

Accepted Manuscript

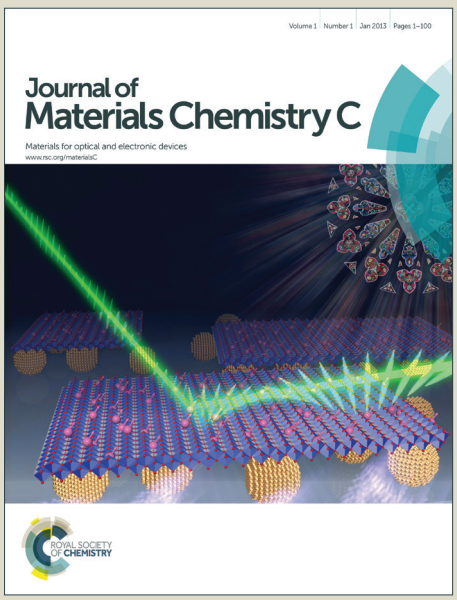

ROYAL SOCIETY OF CHEMISTRY

www.rsc.org/materialsC

Cite this: DOI: 10.1039/c0xx00000x

www.rsc.org/xxxxxx

ARTICLE TYPE

Propeller-like D-π-A architectures: Bright Solid Emitter with AIEE Activity and Large Two-Photon Absorption

Wei Huang[a], Huan Wang[a], Lu Sun[b], Bo Li[c], Jianhua Su*[a] and He Tian*[a]

Received (in XXX, XXX) Xth XXXXXXXXX 20XX, Accepted Xth XXXXXXXXX 20XX

DOI: 10.1039/b000000x

Two novel molecules **TABzPA** and **TATpPA** with D-π-A structure and large π-conjugation have been synthesized via Wittig reaction. Unlike common molecules with aggregation-caused quenching (ACQ) phenomenon, **TABzPA** and **TATpPA** exhibit aggregation-induced emission enhancement (AIEE) activity: weak luminescence in common solvents but strong emission when aggregated as nanoparticles and solid powders. Due to their intramolecular charge transfer (ICT) attribution and AIEE features, **TABzPA** and **TATpPA** display bathochromic effect. Combining ICT and AIEE features, these molecules are intensely yellow solid emitters with high quantum efficiencies about 23.2 % and 24.1 %. Moreover, **TABzPA** and **TATpPA** have excellent two-photon absorption (2PA) property owing to good planarity and large π-conjugation. The values of 2PA cross sections at 800 nm are 7590 GM and 7648 GM. The excellent optical properties of **TABzPA** and **TATpPA** pave the way for future potential applications in bio-photonics and optoelectronics.

Introduction

In recent years, the organic materials with large two-photon absorption (2PA) have drawn much attention due to their photonics and bio-photonics applications, such as 3D data storage,[1] up-converted lasing,[2] power limiting materials,[3] two-photon bio-imaging[4] and so forth. A series of new compounds with large 2PA cross sections (σ) have been investigated both experimentally and theoretically to realize their full potential applications.[5] Resulting from the hardworking of scientists in the past fifteen years, the π-conjugated molecules with various archetypes including quasi-linear, multi-branched and dendritic geometries have displayed good 2PA.[6] The solvent polarity, molecular planarity and hydrogen-bonding also can enhance the 2PA.[7]

However, it is necessary for the 2PA materials can soluble or dispersible and remain highly fluorescent in aqueous media for biophotonic applications.[8] Regretfully, high efficiency 2PA materials have suffered from low fluorescence efficiency or aggregation-quenched emission (AQE).[9] To solve this problem, Tang and co-workers have found a series of compounds with Tetraphenylethylene (TPE) which have been shown recently to exhibit significant enhancement of their light emission upon aggregation. The phenomenon was called aggregation-induced emission (AIE).[10] They thought the reason is that the intramolecular vibrational and rotational motions of the molecule was restricted in solid state.[11] So some special 2PA materials that both have large two-photon activity and overcome fluorescence quenching in aggregation have been designed and synthesized. Recently, Prasad and coworkers have synthesized aggregation-enhanced fluorescence and 2PA materials due to the hindering of molecular internal rotation.[7a, 12] Tang also found luminogenic polymer and nanoparticles of AIE and 2PA based on tetraphenylethene.[13] Our group designed and synthesized significant AIE and 2PA compounds with triarylamine as donor and cyano unit as acceptor.[14]

Triphenylamine was widely used as donor in electroactive materials, because of the good electron-donating and transporting capabilities, as well as their special propeller starburst molecular structure.[15] In recent decades 2PA materials with triphenylamine as donor have attracted much attention. Based on last work, we have synthesized two novel compounds using 1,3,5-triazine as acceptor, triphenylamine as donor and changing π-bridge with thiophene instead of benzene.(See Scheme 1). The high electron affinities and symmetrical structure with triazine have made the compounds with good optical and electrical properties. Also the thiophene bridge has given the compounds red shift[16] in the absorption and the 2PA values are higher than last work.[17] It could be expected these compounds have good potential application in electrical materials.[18]

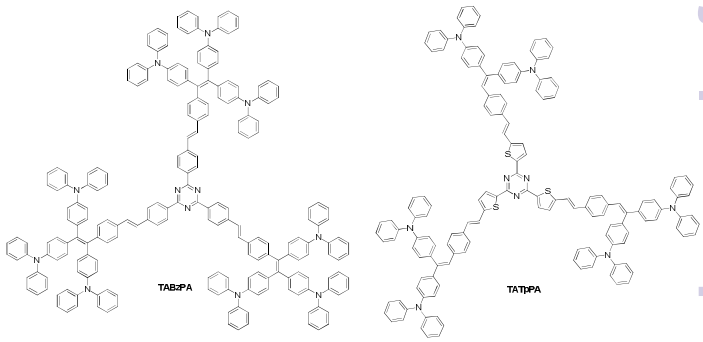

Scheme 1 Molecular structures of **TABzPA** and **TATpPA**

Results and Discussion

Synthesis

The synthetic routes of compounds **TABzPA** and **TATpPA** are shown in Scheme 2. The molecules were prepared via Wittig reaction.[19] The key intermediate compounds **1b** and **2a** were synthesized according to the literature.[17] All of the target compounds were characterized by proton and carbon nuclear magnetic resonance spectroscopy (^{1}H NMR, ^{13}C NMR) and matrix-assisted laser desorption/ionization-time of flight mass spectroscopy (MALDI-TOF) (see the Supporting Information).

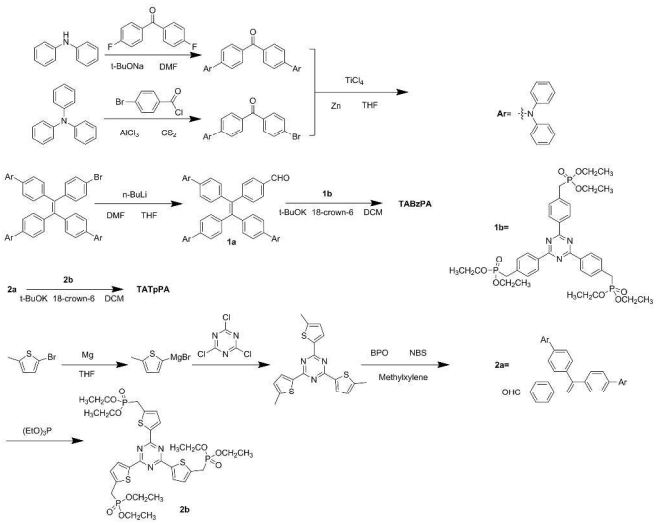

Scheme 2 Synthetic route of compounds **TABzPA** and **TATpPA**

Normalized absorption

The one-photon absorption spectra of **TABzPA** and **TATpPA** in THF are displayed in Figure 1. The peak wavelengths of the compounds are at 426 nm and 445 nm, respectively. The wavelength of **TATpPA** is red shifted by 19 nm compared to **TABzPA**, which owing to the π-bridge of thiophene.

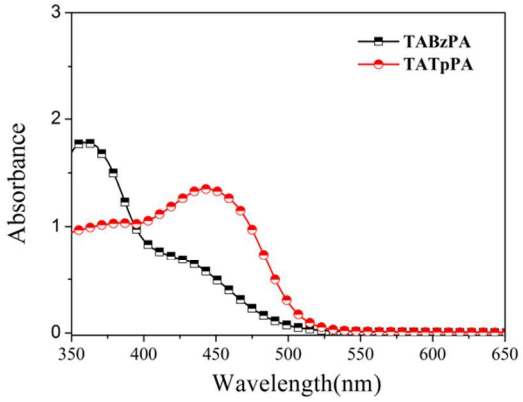

Fig. 1 The one-photon absorption spectra of **TABzPA** and **TATpPA** in THF at the concentration of 1 x 10^{-5} M.

Solvent effect

The solvent effect also can be usually observed in the D-π-A structural molecules. The effect of **TABzPA** and **TATpPA** were investigated by changing the solvent polarity. Figure 2 shows the solvent effect of **TABzPA** and **TATpPA**. We used different solvents by increasing the polarity from cyclohexane to tetrahydrofuran (THF) (losing emission in DMF). For example, the emission of **TABzPA** peaked at 570 nm in cyclohexane and a bathochromic shift to 628 nm in THF. This solvatochromic behaviour is typical for compounds with an internal charge transfer upon excitation and has been fully documented for numerous compounds containing D-π-A structure.[20] Similar phenomenon is observed for **TATpPA**. These solvatochromic results indicate that significant ICT effect exists in these compounds.

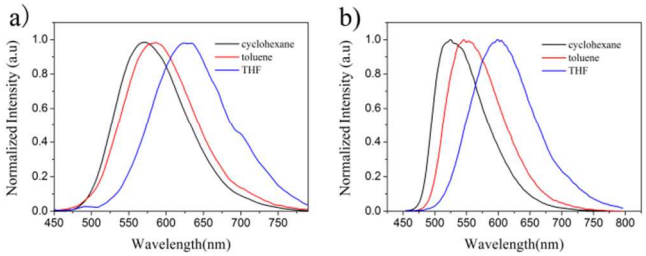

Fig. 2 Normalized emission spectra of **TABzPA** and **TATpPA** in different solvents excited at 428 nm and 450 nm at the concentration of 1 x 10^{-5} M, respectively

AIEE properties

To further investigate the aggregation-induced optical properties of **TABzPA** and **TATpPA**, we employed anhydrous THF as good solvent and water as poor solvent, which is commonly used in the study of AIE or AIEE behaviour. The dispersion of nano-aggregates of **TABzPA** and **TATpPA** were prepared by the precipitation method, adding water to THF solution of the two molecules. For compound **TABzPA**, concentration is kept at 1 x 10^{-5} M. As seen in Figure 3a the fluorescence is weak at water fraction (f_w) ≤ 30 %. When the f_w > 30 %, an obvious enhancement is observed, which is related to the aggregated formation. Finally, when f_w = 80 % the photoluminescence (PL) intensity is boosted to maximum with the peak located at 602 nm, which is similar to the situation when f_w = 90 %. It can indicate that when the f_w = 80 % all the nano-aggregates has all been formed. Definitely, the emission of **TABzPA** is induced by aggregation, thus verifying its AIEE nature. In aggregated state, the intramolecular rotations are restricted, blocking the non-radiative decay path and activate the radiative decay. Therefore the dye gives a strong emitter. However, rotations of the diphenylamine peripheries against the benzene core may effectively deactivate the radiative decay in excited state, resulting in low emission when in the pure solvent.[11] Possibly due to crystallization of the dye, a strong and blue-shifted emission of the aggregates was exhibited.[21]

Figure 3c shows the absorption of **TABzPA** in solution and aggregation. In the nano-aggregate form (f_w = 90 %) the absorption is obviously broadened (λ_{max} = 442 nm), which red-shift by 17 nm compared with solution (λ_{max} = 425 nm). A quantitative I/I_0 is made by calculated the integrands of the PL spectra in different of f_w. The PL intensity of **TABzPA** is weak when the f_w < 20 %, but increased swiftly when f_w > 20 %. At f_w =

90 % the intensity reached highest value, with a 53-fold increase (See Figure 3b). The formation of the nano-aggregates can be certificated by scanning electron microscopy (SEM) (see Figure 4). It reveals that a nano-aggregated structure of the molecule has been formed in high water content. Similar phenomenon is observed for **TATpPA** and they show AIEE performance.

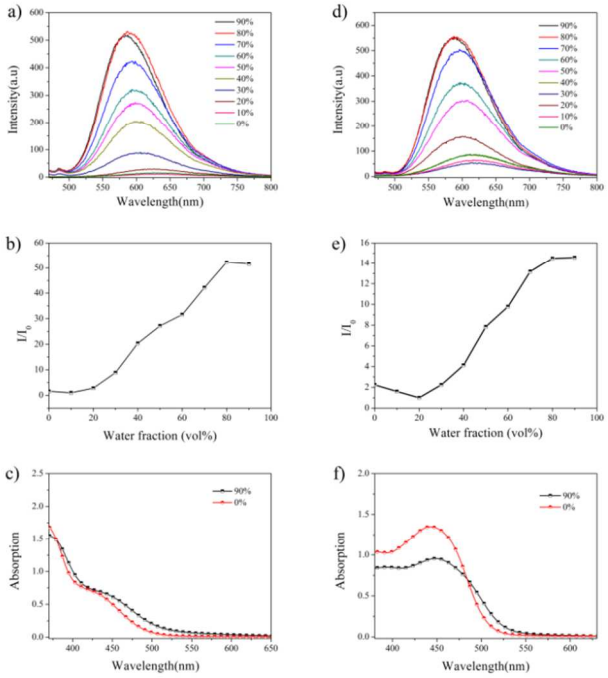

Fig. 3 a), d). The PL spectra of **TABzPA** and **TATpPA** excited at 428 nm and 450 nm, respectively, in different water fraction (f_w) at concentration of 1 x 10^{-5} M. b), e) Plot of (I/I_0) values versus water content of the solvent mixture for **TABzPA** and **TATpPA**. c), f) The absorptions of **TABzPA** and **TATpPA** in THF and f_w = 90 % at concentration of 1 x 10^{-5} M.

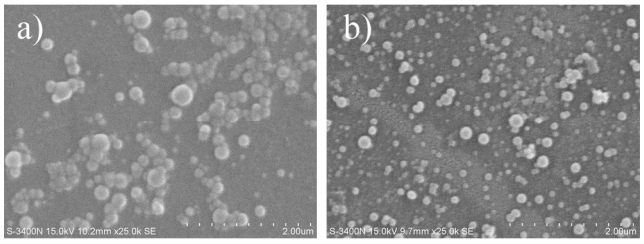

Fig. 4 SEM images of **TABzPA** and **TATpPA**, nano-aggregates were prepared in f_w = 90 % at concentrations of 1x10^{-5} M, respectively.

To further investigate the solvent effect of AIEE, the aggregated states were studied in the other two conditions (THF-cyclohexane and DMF-ethanol). The emission spectra in different mixtures are shown in Figure 5. For **TABzPA**, the PL intensity increases when the cyclohexane fraction (f_{CYH}) ≥ 30 % and the wavelength of emission (λ_{em}) is blue-shifted with the increase of f_{CYH} (from 585 nm to 531 nm). It signifies the polarity of the solution decrease when cyclohexane is added and the nano-aggregates are formed at a high f_{CYH}. Both of the above mechanisms give significant effect for the enhanced emission. For the DMF-ethanol mixture, the PL intensity is very low when ethanol fraction (f_{EtOH}) < 80 %, it is due to DMF is a strong polarity solvent. When the nano-aggregates are formed absolutely in f_{EtOH} = 90 %, the mixture gives a strong emission. The similar phenomenon also can be observed in **TATpPA.**

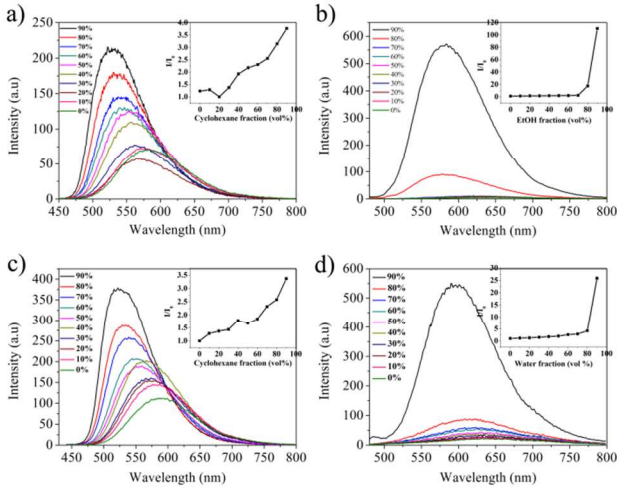

Fig. 5 Emission spectra of **TABzPA** and **TATpPA** (excited at 428 nm and 450 nm, respectively.) in different mixture (a, c THF-cyclohexane and b, d DMF-ethanol) at the concentration of 1 x 10^{-5} M, respectively. Inset is the Plot of (I/I_0) values in different ratio of poor solvent for **TABzPA** and **TATpPA** at the concentration of 1 x 10^{-5} M, respectively.

For biophotonic applications, the bioimaging of HeLa cells have been taken. Figure 6 shows the cell imaging carried out by confocal laser scanning microscopy (CLSM). It indicates the bulkiness molecules are suitable for the biophotonic applications. However, **TATpPA** have better ability of cell imaging than **TABzPA**. This is because of the smaller size of nanoparticle when aggregate in water (see SEM images Figure 4). Also such bulkiness molecules encapsulated in a mixture of DSPE-PEG_{2000} and DSPE-PEG_{5000}-Folate can be applied in targeted cancer cell imaging.[29]

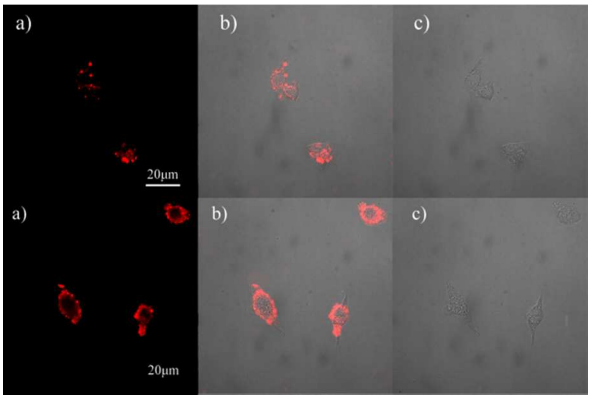

Fig. 6 Cell imaging of **TABzPA** (top) and **TATpPA** (bottom) in HeLa cells a) 450 nm excitations b) overlap of image a and b c) bright field.

Solids Optical properties

Vivid images of the solid powders can intuitively manifest the AIEE attribute. Figure 7 shows the emission spectra of compounds **TABzPA** and **TATpPA** in solid state. The solid powders were recrystallized by toluene. All dyes exhibit intense fluorescence under 365 nm light illumination (see insert images in Figure 7), which peaks are located at 595 nm and 612 nm, respectively. To quantitatively evaluate the fluorescent materials,

the quantum efficiencies (Φ_F) of the solid were investigated. The values of Φ_F were determined to be 23.2 % and 24.1 %, respectively. The high Φ_F values make them potential candidates in OLEDs.[22]

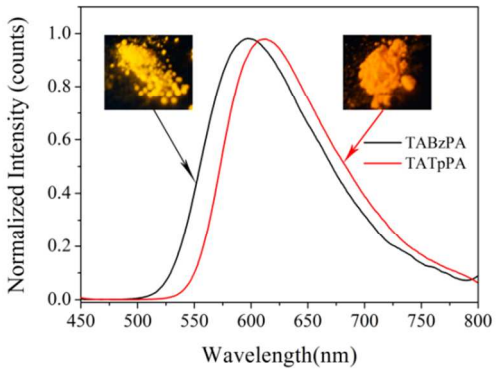

Fig. 7 The normalized emission spectra of **TABzPA** and **TATpPA** as solid powder. Insert images are **TABzPA** and **TATpPA** as solid powders under 365 nm light illumination.

Two-photon absorption properties

2PA cross sections of the **TABzPA** and **TATpPA** were determined by femtosecond open aperture Z-scan technique according to a previously described method and calculated by using the equation $\sigma = h\nu\beta/N_0$, where $N_0=N_AC$ is the number density of the absorption centers, N_A is the Avogadro constant, and C is the concentration of the solution.[23] Figure 8 shows the two-photon fluorescence (2PF) under different excited power density. Attribute to AIEE effect the intensity is low; however, there is a linear relationship between the square of power density (I^2) and the fluorescence intensity. It proves the phenomenon is a process of 2PF.[24] Figure 9 is the data fitting of the open-aperture Z-scan. The 2PA cross section values of **TABzPA** and **TATpPA** are 7590 GM and 7648 GM, respectively, at wavelength of 800 nm. These values are higher than so many other materials.[25] Otherwise we have once reported a molecular **3c** (see SI Figure 8), whose value is 5782 GM. The increase of the 2PA value is due to the improvement of the donor and π bridge of molecular structure.

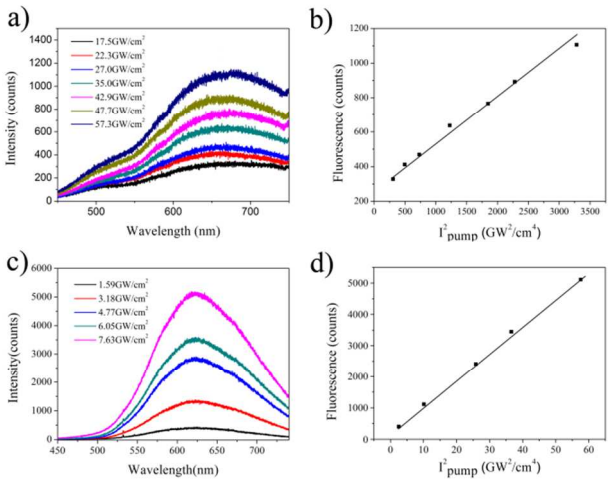

Fig. 8 a), c) The emission spectra of **TABzPA** and **TATpPA** in different excited power density of 800 nm pulse in THF. b), d) The relationship between the square of power density (I^2) and the fluorescence intensity.

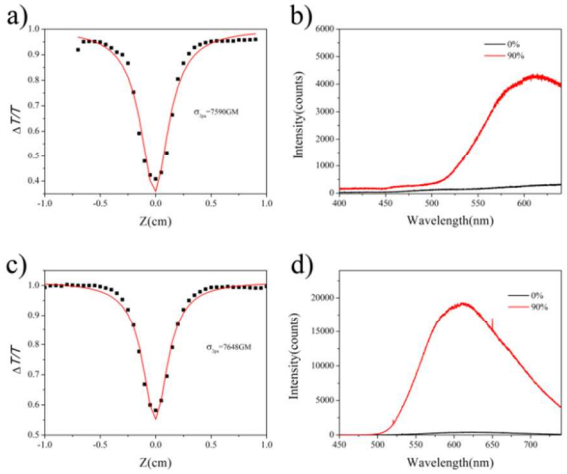

Fig. 9 a), c) Open-aperture Z-scan trace of **TABzPA** and **TATpPA** (scattered circles= experimental data, read line = theoretical fitted data). b), d) The TPF emission spectra of **TABzPA** and **TATpPA** in the mixture solution (f_w= 90 %) at a concentration of $1x10^{-5}$ M excited at 800 nm laser, respectively.

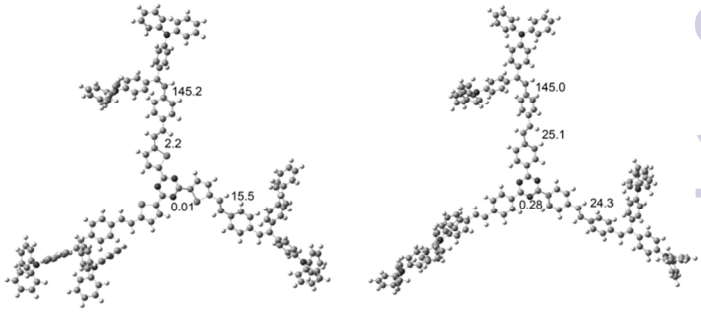

Fig. 10 The dihedral angle of **TATpPA** and **3c** by calculation.

For a better explanation of the large 2PA cross sections, we have calculated the molecular structures. The optimized geometry is achieved through Density functional theory (DFT) at the B3LYP level together with a minor basis set 3-21G. The Figure 10 shows the calculated dihedral angle of the molecules. The angle between triazine and thiophene of **TATpPA** is 0.01°, which is similar to **3c** (the angle between triazine and benzene is 0.28°). However, the angle of the π-bridge is different: the angle of **TATpPA** between thiophene and ethylenic bond is 15.5°, which is smaller than **3c** (the angle of **3c** is 24.3°). The small angle make the **TATpPA** have better planarity than **3c**, so **TATpPA** have better 2PA cross section value.[26] Moreover, due to the better electronic ability and larger π-conjugated system, the **TABzPA** shows larger 2PA cross section value.[27] The two-photon fluorescence (TPF) has been examined for investigating the aggregation effect on the two-photon activity (see Figure 9). All dyes exhibit yellow fluorescence with peaks located at 611 nm and 615 nm in mixture solvent (f_w = 90 % THF and water) under the excitation of 80 fs, 800 nm pulse. Figure 11 shows the one- and two-photon emission images in different water fractions of solution. There is weak emission in pure THF, while in the solutions of f_w = 90 % the dyes irradiate yellow emission. Due to

the limitation of our laser apparatus, only irradiation at the wavelength of 800 nm was used to carry out the two-photon excitation experiment. The 2PA cross sections for **TABzPA** and **TATpPA** would be better in other wavelengths.

Fig. 11 a) The one-photon fluorescence (OPF) emission photos of **TABzPA** and **TATpPA** at a concentration of $1x10^{-5}$ M, respectively, in different ratio of water in THF under 365 nm light illumination. b) The two-photon emission (TPF) emission images of **TABzPA** and **TATpPA**, respectively, in the different ratio of water in THF excited at 800 nm laser.

Conclusion

With combination of arylamines and triazine in typical propeller-like D-π-A architectures, two novel molecules **TABzPA** and **TATpPA** have been synthesized. Both compounds display AIEE phenomenon: practically weak luminescence when dissolved in solvents but emit intensely upon aggregate formation. The solid quantum efficiencies are 23.2 % and 24.1 % due to the AIEE and ICT attributes. The good planarity and large π-conjugation make all molecules exhibit aggregation-enhanced two-photon fluorescence (2PF) and excellent two-photon absorption (2PA). Their values of 2PA cross section at 800 nm are 7590 GM and 7648 GM. The excellent 2PA and solid quantum efficiencies pave the way for use in potential fluorescence materials.

Experimental Section

Instruments

^{1}H and ^{13}C NMR spectra were measured on Bruker AM-400 spectrometer using d-chloroform as solvent and tetramethylsilane (TMS, δ = 0 ppm) as internal standard. The UV/Vis spectra were recorded on a Nicolet CARY 100 spectrophotometer. The PL spectra were taken on a Varian-Cary fluorescence spectrophotometer. The quantum yield for solid powders was measured by Quanta-φ F-3029 Integrating Sphere. The 2PA cross sections were measured by a femtosecond open-aperture Z-scan technique according to a previously described method. The TPF was achieved using femtosecond pulses with different intensities at a wavelength of 800 nm. The repetition rate of the laser pulses was 250 KHz and the pulse duration was 80 fs.

Materials

THF was pre-dried over sodium for 24h and then redistilled under argon atmosphere sodium benzophenone ketyl prior to use. DMF was refluxed with calcium hydride and distilled before use. Starting materials bis(4-fluorophenyl) methanone and diphenylamine were obtained from commercial sources (J&K, Aldrich), and used without further purification. The key intermediate compounds were prepared according to the previous published procedures.[28]

Synthesis

bis(4-(diphenylamino)phenyl)methanone: For a three-neck flask diphenylamine 6.2 g (36.7 mmol), sodium tert-butoxide 5.28 g (55 mmol) dissolved into 100 ml anhydrous DMF, slowly drop bis(4-fluorophenyl) methanone 4 g (18.3 mmol) of 50ml anhydrous DMF solution under N^2 atmosphere in 1h. The reaction mixture was refluxed for 10h, upon cooling the mixture was poured into 200 ml ice water, then a deep yellow solid precipitate was filtered off, washed with ethanol. After vacuum drying have got 7.85 g yellow solid. Yield: 83 %; ^{1}H NMR (400 MHz, $CDCl_3$, TMS), δ = 7.74 (m, 4H), 7.35 (m, 8H), 7.22 (m, 8H), 7.14 (m, 4H), 7.02 (d, *J* = 8.8 Hz, 4H).

(4-bromophenyl)(4-(diphenylamino)phenyl)methanone: In a 250 ml three-neck flask, 6.7g (27 mmol) dissolving 60 ml CS_2. Slowly add $AlCl_3$ 4.6g (34.5 mmol) at 0°C and stirred 30 min under N_2 atmosphere. Dissolving 4-bromobenzoyl chloride 5g (22.8 mmol) in 50 ml CS_2, then dropped into the flask. After reaction mixture for 8h at 0°C, the mixture was poured into 200 ml water and extracted with DCM (50 ml X 3). The combined organic layer was washed with water, dried with anhydrous $MgSO_4$. The resident was purified by column chromatography on silica (PE: DCM = 3:1) to give a yellow solid 7.41 g. Yield: 76 %; ^{1}H NMR (400MHz, $CDCl_3$, TMS), δ = 7.72 (m, 5H), 7.33 (t, *J* = 7.8 Hz, 5H), 7.18 (d, *J* = 7.5 Hz, 6H), 7.00 (d, *J* = 8.8 Hz, 2H).

4,4',4''-(2-(4-bromophenyl)ethene-1,1,2-triyl)tris(N,N-diphenylaniline): In a 100 ml three-neck flask, Zn 1.5g (23 mmol) added in 40ml anhydrous THF. At -10°C, injected $TiCl_4$ 2.5ml (23 mmol) under N_2 atmosphere. The mixture stirred for 3h under refluxing, then slowly dropped bis(4-(diphenylamino) phenyl) methanone 3g (5.8 mmol) mixed with (4-bromophenyl) (4-(diphenylamino) phenyl) methanone 1g (2.3 mmol) solution of THF. The reaction mixture was refluxed for 4h, upon cooling the mixture was poured into 150 ml ice water. After filtrating, the filter washed by DCM. The combined organic layer was washed with water, dried over with anhydrous $MgSO_4$. The resident was purified by column chromatography on silica (PE: DCM = 4:1) to give a light yellow solid 1.01 g. Yield: 48 %; ^{1}H NMR (400MHz, $CDCl_3$, TMS), δ = 7.31 - 7.16 (m, 13H), 7.12 - 6.93 (m, 23H), 6.90 - 6.76 (m, 10H). HRMS (m/z): [M]+ calcd for C62H47N3Br, 912.2953; found, 912.2957.

4-(1,2,2-tris(4-(diphenylamino)phenyl)vinyl)benzaldehyde (1a): For a 50 ml Schlenk reactor, 1.01g (1.1 mmol) 4,4',4''-(2-(4-bromophenyl)ethene-1,1,2-triyl)tris(N,N-diphenylaniline) dissolved in 30ml anhydrous THF at -78°C. After 30 min injected 0.6ml 2.4 mol/l n-BuLi in hexane. After 1h, added 0.23 g (3.3 mmol) anhydrous DMF and stirred for 2h under N_2 atmosphere. Then taken the reactor out and stirred overnight at room temperature. Poured the mixture into water and extracted with DCM (30 ml X 3). The combined organic layer was washed with water and was dried over anhydrous $MgSO_4$, concentrated using a rotary evaporator. The resident was purified by column chromatography on silica (PE: DCM= 2:1) to give a yellow solid 0.71 g. Yield: 75 %; ^{1}H NMR (400 MHz, $CDCl_3$, TMS), δ = 9.82 (s, 1H), 7.92 - 7.79 (m, 4H), 7.24 - 7.13 (m, 20H), 6.81 - 6.69 (m, 24H).

2,4,6-tris(5-methylthiophen-2-yl)-1,3,5-triazine: For a 250 ml three-neck flask, added 0.81g (33.8 mmol) Mg, 15ml anhydrous THF and a grain of iodine. 5g (28.1 mmol) 2-bromo-5-methylthiophene dissolved in 50 ml anhydrous THF, dropped a few solution in the flask. All solution was dropped slowly under N_2 atmosphere when the reaction was caused. After stirring 2h at RT, 1.73g (9.37mmol) 2,4,6-trichloro-1,3,5-triazine dissolving in 50 anhydrous THF was dropped, the mixture refluxed for 10h. Poured the mixture into water and extracted with DCM (50 ml X 3). The combined organic layer was washed with water and was dried over anhydrous $MgSO_4$, concentrated using a rotary evaporator. The resident was purified by column chromatography on silica (PE: DCM= 3: 1) to give a light solid 2.8 g. Yield: 81 %; ^{1}H NMR (400MHz, $CDCl_3$, TMS), δ = 8.05 (d, *J*=3.7, 3H), 6.88 (d, *J*=3.5, 3H), 2.58 (s, 9H).

Hexaethyl((5,5',5''-(1,3,5-triazine-2,4,6-triyl)tris(thiophene-5,2-diyl))tris(methylene))tris(phosphonate) (2b): In a 100 ml round-bottom flask, 2,4,6-tris(5-methylthiophen-2-yl)-1,3,5-triazine 2g (5.4 mmol), 5.34

g NBS (17.1 mmol) and BPO (0.3 g, 1.2 mmol) were dissolved into 50 ml chlorobenzene and heated at 110 °C for 8h. The mixture was filtered and the solvent was removed under vacuum. The resident was dissolved into 10 ml triethyl phosphite and refluxed for 10h. The excessive trimethyl phosphite was removed under vacuum. The residue was purified by column chromatography on silica with EA to afford the product as a white powder 2.43 g. Yield: 58 %; ^{1}H NMR (400 MHz, $CDCl_3$, TMS), δ = 8.10 (d, *J*=12.1,3H), 7.10 (t, *J*=3.6, 3H), 4.12 (dt, *J*=14.3, 7.1, 12H), 3.43 (d, *J*=21.5, 6H), 1.31 (t, *J*=7.1, 18H).

TABzPA: In a 25 ml flask, 600 mg (0.74 mmol) **1a**, 170 mg (0.22 mmol) 1b, 124 mg (1.11 mmol) t-BuOK and 18-crown-6 (20 mg, 0.08 mmol), and 100ml DCM under N_2 atmosphere. The mixture was stirred at 45 °C for 12h. Upon cooling poured the mixture into water and extracted with DCM (30 ml x 3). The combined organic layer was washed with water and was dried over anhydrous $MgSO_4$, concentrated using a rotary evaporator. The resident was purified by column chromatography on silica (PE: DCM=4:1 v/v) to give a deep yellow solid 285 mg. Yield: 45 %; ^{1}H NMR (400 MHz, $CDCl_3$, TMS), δ = 8.78 (d, *J*=8.4, 6H), 7.71 (d, *J*=8.4, 6H), 7.38 (d, *J*=8.3, 6H), 7.25 – 7.20 (m, 36H), 7.14 (d, *J*=8.2, 6H), 7.07 (t, *J*=7.2, 36H), 7.03 – 6.91 (m, 42H), 6.89 – 6.81 (m, 18H). ^{13}C NMR ($CDCl_3$, 100 MHz, TMS), 121.07, 122.81, 122.99, 123.08, 123.54, 124.48, 124.60, 125.89, 127.11, 128.34, 129.28, 129.91, 130.83, 131.27, 134.08, 134.42, 136.86, 138.14, 139.02, 142.39, 147.14, 147.44, 147.52, 147.59, 149.73, 168.90, 170.56. MALDI-TOF: [M] Calcd for $C_{213}H_{156}N_{12}$: 2881.2576, Found: 2881.2582.

TATpPA: In a 25ml flask, 618 mg (1 mmol) **2a**, 257 mg (0.33 mmol) **2b**, 168 mg (1.5 mmol) t-BuOK and 18-crown-6 (20 mg, 0.08 mmol), and 100ml DCM under N_2 atmosphere. The mixture was stirred at 45 °C for 12h. Upon cooling poured the mixture into water and extracted with DCM (30 ml x 3). The combined organic layer was washed with water and was dried over anhydrous $MgSO_4$, concentrated using a rotary evaporator. The resident was purified by column chromatography on silica (PE: DCM=4:1 v/v) to give a deep yellow solid 365 mg. Yield: 51 %; 1H NMR (400 MHz, CDCl3), δ = 8.14 (d, *J*=3.9, 3H), 7.37 – 7.30 (m, 21H), 7.24 - 7.27(m, 10H), 7.23 – 6.99 (m, 74H), 6.91 (s, 3H). ^{13}C NMR ($CDCl_3$, 100 MHz, TMS), 121.10, 122.84, 123.01, 123.57, 124.63, 125.92, 126.30, 127.13, 128.37, 129.31, 130.86, 131.29, 132.52, 134.11, 134.45, 136.89, 138.17, 139.05, 142.41, 147.18, 147.47, 147.55, 147.62, 149.75, 168.93, 170.56. MALDI-TOF: [M] Calcd for $C_{153}H_{111}N_9S_3$: 2169.8125, Found: 2169.8143.

Acknowledgements

This work was supported by NSFC/China and the National Basic Research 973 Program.

Notes and references

[a] *Key Laboratory for Advanced Materials and Institute of Fine Chemicals, East China University of Science & Technology, Shanghai, 200237, China. E-mail:tianhe@ecust.edu.cn; Fax: +86-21-64252756; Tel: +86-21-64252756*

[b] *Department of Theoretical ChemistrySchool of Biotechnology, Royal Institute of Technology, S-10691 Stockholm, Sweden*

[c] *Key Laboratory of Polar Materials and Devices, Ministry of Education, East China Normal University, Shanghai 200241, China*

1 a) C. C. Corredor, Z.. L. Huang, K and D. Belfield, *Adv. Mater.,* 2006, **18**, 2910-2914; b) C. C. Corredor, Z. L. Huang, K. D. Belfield, A. R. Morales and M. V. Bondar, *Chem. Mater.,* 2007, **19**, 5165-5173.

2 a) A. Mukherjee, *Appl. Phys. Lett.,* 1993, **62**, 3423-3425; b) H. M. Kim and B. R. Cho, *Acc. Chem. Res.,* 2009, **42**, 863-872; c) C. C. Lin, M. Velusamy, H. H. Chou, J. T. Lin and P. T. Chou, *Tetrahedron,* 2010, **66**, 8629-8634; d) Y. Jiang, Y. Wang, B. Wang, J. Yang, N. He, S. Qian and J. Hua, *Chem. Asian J.,* 2011, **6**, 157-165.

3 a) T. Brixner, N. Damrauer, P. Niklaus and G. Gerber, *Nature,* 2001, **414**, 57-60; b) J. Ehrlich, X. Wu, I. Lee, Z. Y. Hu, H. Röckel, S. Marder and J. Perry, *Opt. Lett.,* 1997, **22**, 1843-1845; c) B. Li, Z. Li, and J. Hua, *Science China: Chemistry*, 2013, **56**, 1204-1212.

4 W. Denk, J. H. Strickler and W. W. Webb, *Science,* 1990, **248**, 73-76.

5 M. Pawlicki, H. A. Collins, R. G. Denning and H. L. Anderson, *Angew. Chem. Int. Ed.* 2009, **48**, 3244-3266.

6 a) R. Hu, J. L. Maldonado, M. Rodriguez, C. Deng, C. K. W. Jim, J. W. Y. Lam, M. M. F. Yuen, G. Ramos-Ortiz and B. Z. Tang, *J. Mater. Chem.,* 2012, **22**, 232-240; b) S. Yao and K. D. Belfield, *Eur. J. Org. Chem.,* 2012, 3199-3217.

7 H. Myung Kim and B. Rae Cho, *Chem.Commun.,* 2009, 153-164.

8 a) S. Kim, Q. Zheng, G. S. He, D. J. Bharali, H. E. Pudavar, A. Baev and P. N. Prasad, *Adv. Funct. Mater.,* 2006, **16**, 2317-2323; b) W. Qin, D. Ding, J. Liu, W. Z. Yuan, Y. Hu, B. Liu and B. Z. Tang, *Adv. Funct. Mater.,* 2012, **22**, 771-779.

9 A. Schiller, R. A. Wessling and B. Singaram, *Angew. Chem.,* 2007, **119**, 6577-6579.

10 a) J. Luo, Z. Xie, J. W. Y. Lam, L. Cheng, H. Chen, C. Qiu, H. S. Kwok, X. Zhan, Y. Liu, D. Zhu and B. Z. Tang, *Chem. Commun.,* 2001, 1740-1741; b) Y. Liu, S. Chen, J. W. Y. Lam, F. Mahtab, H. S. Kwok and B. Z. Tang, *J. Mater. Chem.,* 2012, **22**, 5184-5189.

11 Y. Hong, J. W. Y. Lam and B. Z. Tang, *Chem. Commun.,* 2009, 4332-4353.

12 S. Kim, T. Y. Ohulchanskyy, H. E. Pudavar, R. K. Pandey and P. N. Prasad, *J. Am. Chem. Soc.,* 2007, **129**, 2669-2675.

13 T. Wang, Y. Cai, Z. Wang, E. Guan, D. Yu, A. Qin, J. Sun and B. Z. Tang, C. Gao, *Macromol. Rapid Commun.,* 2012, **33**, 1584-1589.

14 B. Wang, Y. Wang, J. Hua, Y. Jiang, J. Huang, S. Qian and H. Tian, *Chem. Eur. J.,* 2011, **17**, 2647-2655.

15 Z. Ning and H. Tian, *Chem. Commun.,* 2009, 5483-5495.

16 K. R. Justin Thomas, Y. C. Hsu, J. T. Lin, K. M. Lee, K. C. Ho, C. H. Lai, Y. M. Cheng and P. T. Chou, *Chem. Mater.,* 2008, **20**, 1830-1840.

17 W. Huang, F. Tang, B. Li, J. Su and H. Tian, *J. Mater. Chem. C,* 2014, **2**, 1141-1148.

18 C. Le Droumaguet, A. Sourdon, E. Genin, O. Mongin and M. Blanchard-Desce, *Chem. Asian J.,* 2013, **8**, 2984-3001.

19 G. A. Sotzing, C. A. Thomas, J. R. Reynolds and P. J. Steel, *Macromolecules,* 1998, **31**, 3750-3752.

20 F. S. Kim, X. Guo, M. D. Watson and S. A. Jenekhe, *Adv. Mater.,* 2010, **22**, 478-482.

21 Z. Zhang, B. Xu, J. Su, L. Shen, Y. Xie and H. Tian, *Angew. Chem. Int. Ed.*, 2011, **50**, 11654-11657.

22 (a) W. Z. Yuan, Y. Gong, S. Chen, X. Y. Shen, J. W. Y. Lam, P. Lu, Y. Lu, Z. Wang, R. Hu, N. Xie, H. S. Kwok, Y. Zhang, J. Z. Sun and B. Z. Tang, *Chem. Mater.,* 2012, **24**, 1518-1528; (b) J. Huang, R. Tang, T. Zhang, Q. Li, G. Yu, S. Xie, Y. Liu, S. Ye, J. Qin and Z. Li, *Chem. Eur. J.,* 2014, **20**, 5317-5326. (c) J. Huang, N. Sun, P. Chen, R. Tang, Q. Li, D. Ma and Z. Li, *Chem. Commun.*, 2014, **50**, 2136-2138.

23 J. L. Hua, B. Li, F. S. Meng, F. Ding, S. X. Qian and H. Tian, *Polymer,* 2004, **45**, 7143-7149.

24 G. S. He, L. S. Tan, Q. Zheng and P. N. Prasad, *Chem. Rev*., 2008, **108**, 1245-1330.

25 (a) B. Xu, J. Zhang, H. Fang, S. Ma, Q. Chen, H. Sun, C. Im and W. Tian, *Polym. Chem.,* 2014, **5**, 479-488. (b) B. Xu, J. He, Y. Liu, B. Xu, Q. Zhu, M. Xie, Z. Zheng, Z. Chi, W. Tian, C. Jin, F. Zhao, Y. Zhang and J. Xu, *J. Mater. Chem. C*, 2014, **2**, 3416-3428.

26 S. Lee, K. R. J. Thomas, S. Thayumanavan and C. J. Bardeen, *J. Phys. Chem. A* 2005, **109**, 9767-9774.

27 T. C. Lin, Y. H. Lee, C. Y. Liu, B. R. Huang, M. Y. Tsai, Y. J. Huang, J. H. Lin, Y. K. Shen and C. Y. Wu, *Chem. Eur. J.,* 2013, **19**, 749-760.

28 Z. Yang, Z. Chi, B. Xu, H. Li, X. Zhang, X. Li, S. Liu, Y. Zhang and J. Xu, *J. Mater. Chem.,* 2010, **20**, 7352-7359.

29 K. Li, Y. Jiang, D. Ding, X. Zhang, Y. Liu, J. Hua, S.-S. Feng and B. Liu, *Chem. Commun.*, 2011, **47**, 7323-7325.